Geology

The thickness of subduction plate boundary faults from the seafloor into the seismogenic zone

Christie D. Rowe, J. Casey Moore, Francesca Remitti and the IODP Expedition 343/343T Scientists

Geology 2013;41;991-994
doi: 10.1130/G34556.1

Notes

The thickness of subduction plate boundary faults from the seafloor into the seismogenic zone

Christie D. Rowe[1]*, J. Casey Moore[2], Francesca Remitti[3], and the IODP Expedition 343/343T Scientists[4]
[1]Department of Earth and Planetary Sciences, McGill University, 3450 University Street, Montréal, Québec H2A 0E8, Canada
[2]Department of Earth & Planetary Sciences, University of California, 1156 High Street, Santa Cruz, California 95064, USA
[3]Dipartimento di Scienze Chimiche e Geologiche, University of Modena and Reggio Emilia, largo S. Eufemia, 19 - 41125 Modena, Italy
[4]Integrated Ocean Drilling Program, Japan Trench Fast Drilling Project (JFAST), 1 April–24 May 2012 and 5–19 July 2012; see the GSA Data Repository (see text footnote 1) for a list of participants.

ABSTRACT

The thickness of an active plate boundary fault is an important parameter for understanding the strength and spatial heterogeneity of fault behavior. We have compiled direct measurements of the thickness of subduction thrust faults from active and ancient examples observed by ocean drilling and field studies in accretionary wedges. We describe a general geometric model for subduction thrust décollements, which includes multiple simultaneously active, anastomosing fault strands tens of meters thick. The total thickness encompassing all simultaneously active strands increases to ~100–350 m at ~1–2 km below seafloor, and this thickness is maintained down to a depth of ~15 km. Thin sharp faults representing earthquake slip surfaces or other discrete slip events are found within and along the edges of the tens-of-meters-thick fault strands. Although flattening, primary inherited chaotic fabrics, and fault migration through subducting sediments or the frontal prism may build mélange sections that are much thicker (to several kilometers), this thickness does not describe the active fault at any depth. These observations suggest that models should treat the subduction thrust plate boundary fault as <1–20 cm thick during earthquakes, with a concentration of postseismic and interseismic creep in single to several strands 5–35 m thick, with lesser distributed interseismic deformation in stratally disrupted rocks surrounding the fault strands.

INTRODUCTION

The thickness of plate boundary faults is a key parameter for understanding mechanical behavior (Sibson, 2003). For any increment of slip, the width over which deformation is distributed determines the strain rate in the fault rock, which controls the activity of different deformation mechanisms. At high slip rates, a moderately narrow slip surface may be heated by friction to cause thermal pressurization, while the same amount of slip distributed over a thinner fault core may undergo frictional melting, causing melt lubrication. Fault thickness affects other physical parameters that control dynamic processes. Porosity and permeability variations during the seismic cycle scale with fault width (Sleep and Blanpied, 1992), as do dilation-related controls on changing fault strength (Segall and Rice, 1995).

Determination of décollement thickness has relied mostly on seismic reflection imaging (Bangs et al., 2004; Shipley et al., 1994). Seismic imaging and some outcrop studies reveal reflective or deformed zones tens of meters to kilometers thick, but it is difficult to determine whether these are representative of the instantaneously active fault or built progressively through multiple stages of deformation, and therefore overestimate fault thickness (Cowan, 1978; Vannucchi et al., 2012; Wakabayashi, 2011). Seismic reflection imaging has differentiated layers of low impedance, and probably high pore pressure, tens of meters thick within thicker deformed zones (e.g., Bangs et al., 2004; Shipley et al., 1994). These may correlate to zones of active shearing or a zone of fluid trapped beneath a shearing layer.

This paper focuses only on the plate boundary fault strands (geologically contemporaneous zones accommodating most of the strain of relative plate motion). We do not use the term "subduction channel," which may describe any of a suite of observational and theoretical definitions of the plate boundary zone that may vary substantially in space and time (Vannucchi et al., 2012). We constrain this variation in space by looking at a suite of examples where the width of the deforming zone is precisely measured, and where structural relations suggest preservation of a discrete time period of fault activity.

We have compiled observations of subduction thrust faults active at depths from 0 to 15 km (Fig. 1A; Table 1). From ocean drilling, we compiled direct measurements from core or logging-while-drilling data of the thickness of the décollement offshore Costa Rica, Barbados, southwest Japan, and northeast Japan. The

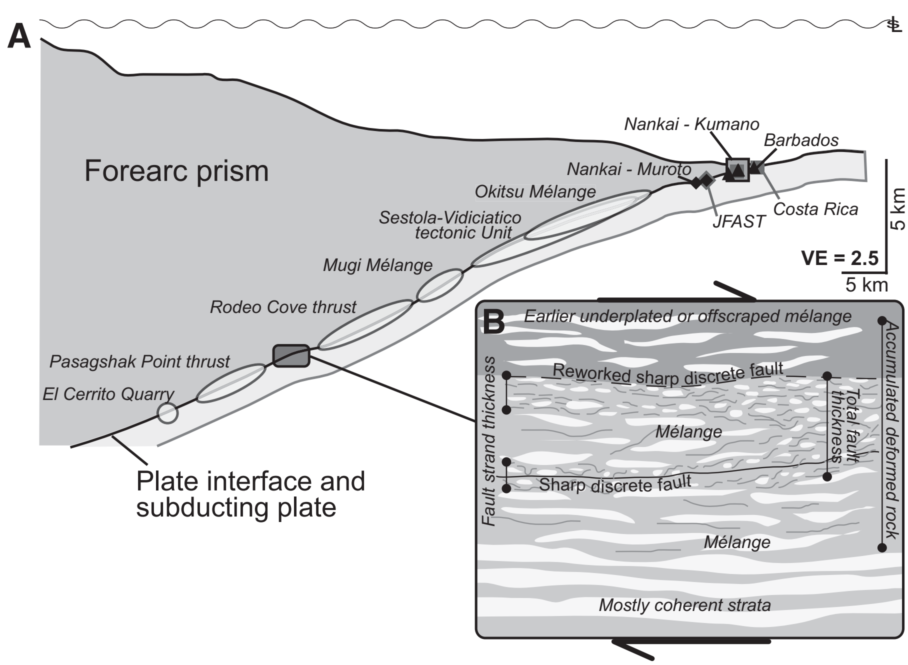

Figure 1. A: Cross section of vertically exaggerated (VE) subduction zone with depth (below seafloor) of representative case studies compiled in this paper. Filled symbols are observations from ocean drilling; ellipses are data from on-land geological observations including depth uncertainty range. B: Fault zone thickness definitions used in this compilation. Although total thickness of deformed rock may exceed total fault thickness, we measure only deforming thickness simultaneously active at depth of interest. JFAST—Japan Trench Fast Drilling Project.

*E-mail: christie.rowe@mcgill.ca.

GEOLOGY, September 2013; v. 41; no. 9; p. 991–994; Data Repository item 2013277 | doi:10.1130/G34556.1 | Published online 3 July 2013

TABLE 1. COMPILED THICKNESS OBSERVATIONS BY DIRECT MEASURE OF GEOLOGICALLY INSTANTANEOUS SHEARING WIDTH FROM OCEAN DRILLING AND OUTCROP OBSERVATIONS OF EXHUMED FAULTS

Location	Depth below seafloor (m)	Total fault zone thickness (m)	Fault strand thickness (m)	Discrete slip surface thickness (m)	Temperature (°C)	Source*
Costa Rica, IODP Leg 170, Site 1043	146	9.07	NR	NR	NR	1
Barbados, IODP Leg 171, Site 1047	276	45	10, 26	N/A	NR	2
Costa Rica, IODP Leg 205 Site 1254	338	45	NR	0.03–0.08	NR	3
Costa Rica, IODP Site 1040	351	24.2	NR	NR	NR	1
Nankai Kumano, IODP Site C0007	398.5	47.5	NR	0.002	NR	4
Barbados, IODP Leg 171, Site 1045 (from LWD)	425	13	NR	NR	NR	2
Barbados, IODP Leg 110, Site 671	500	41	NR	NR	NR	5
Nankai Muroto, IODP Leg 190 Site 1174	807	32.6	NR	N/A	<140	6
Japan Trench, IODP Expedition 343/343T, C00019 (JFAST)	821	<4.87	5	0.001	25	7
Nankai Muroto, IODP Leg 196, Site 808 (LWD)	897	68	6, 6, 5	NR	NR	6
Nankai Muroto, IODP Leg 131, Site 808 (core)	945	19.2	NR	NR	NR	8
Okistsu Mélange, Shikoku Island, Japan	1500–4000	~200	2–5	0.001	190–270	9, 10, 11
Sestola-Vidiciatico tectonic unit, Apennines, Italy	2000–5000	200–500	N/A	0.03	100–150	12, 13, 14
Mugi Mélange, Shikoku Island, Japan (fluidized rock)	6000–7000	100–150	5–30	0.02–0.2	130–150	15, 16, 17
Mugi Mélange, Shikoku Island, Japan (pseudotachylytes)	6000–7000	100–150	1–2	0.001	170–200	11
Rodeo Cove thrust, Franciscan Complex, California	8000–10,000	200	30–50	0.001–0.2	200–250	18
Pasagshak Point thrust, Kodiak, Alaska	12,000–14,000	400	7–31	0.05–0.35	250	19, 20
El Cerrito Quarry thrust, Franciscan Complex, California	~15,000	100–200	10–20	0.001–0.01	250–350	21, 22

Note: IODP—Integrated Ocean Drilling Program; JFAST—Japan Trench Fast Drilling Project; NR—not reported; N/A—not applicable; LWD—logging while drilling. Leg refers to the ocean drilling expedition and Site refers to the specific drill site where measurement was made from core. Depths for ocean drilling measurements are to center of fault zone.

*References: 1—Shipboard Scientific Party (1997), 2—Shipboard Scientific Party (1998), 3—Shipboard Scientific Party (2003), 4—Expedition 316 Scientists (2009), 5—Shipboard Scientific Party (1988), 6—Shipboard Scientific Party (2002), 7—Chester et al. (2012), 8—Shipboard Scientific Party (1991), 9—Ikesawa et al. (2003), 10—Sakaguchi (2003), 11—Ujiie et al. (2007a), 12—Remitti et al. (2007), 13—Vannucchi et al. (2008), 14—Vannucchi et al. (2012), 15—Ujiie et al. (2007b), 16—Ikesawa et al. (2005), 17—Kimura et al. (2012), 18—Meneghini and Moore (2007), 19—Rowe et al. (2011), 20—Rowe et al. (2005), 21—Wakabayashi (2011), 22—Wakabayashi (2013).

depth below seafloor is precisely known (~150–950 m; Fig. 1A). To acquire deeper measurements, we refer to geological studies of exposed thrust faults preserved in ancient subduction complexes in California, Alaska, Italy, and Japan. The depth of activity is estimated from pressure proxies such as fluid inclusion thermobarometry or metamorphic mineral assemblage, and is influenced by assumptions of thermal structure and overburden density. These examples are plotted as depth ranges (Figs. 1A and 2).

FAULT THICKNESS MEASUREMENTS

Over the studied depth range, the plate boundary fault structure can be generally described as one or more intensively sheared fault strands with sharp discrete faults inside or along the edge (Fig. 1B). Some contain pseudotachylyte and are interpreted as earthquake slip surfaces, while the rate of localized slip on others is unknown. If more than one fault strand is simultaneously active, the total fault zone thickness is defined as the minimum structural thickness encompassing all simultaneously active strands. As shear migrates through time, a greater thickness of sheared rock or mélange may accumulate, within which it may be difficult to differentiate the total fault thickness. Mélange may form by flattening and volume loss rather than high shear strain (Fagereng, 2013), or may result from structural overprint on a sedimentary mélange (Cowan, 1978; Vannucchi et al., 2008; Wakabayashi, 2011). Therefore, we do not use estimates of décollement thickness derived from seismic reflection images, as it is impossible to distinguish the active fault zone from the cumulative thickness of sheared rock that may include previously underplated sediments (Fig. 1B), and the resolution of seismic reflection data is many tens of meters (similar to the fault strand thickness). Steep faults cutting the upper plate (splay faults) are contemporaneous with the décollement. Motion on these faults acts to thicken the prism but they are distinct from the décollement that accommodates most of the relative convergence of the plates; we have not included them in our analysis.

All fault strands observed in ocean drilling are assumed to be active, and we reviewed both core and logging data to insure that all faults in the section were counted (Table 1). For the outcrop studies, two criteria were used to establish geologically contemporaneous (10–100 k.y. time scales) fault strands. Multiple faults comprising a duplex structure are assumed to be contemporaneous (Okitsu, southwest Japan; Sestola-Vidiciatico, Italy; Mugi, Japan), and in Sestola-Vidiciatico, identical nanofossil ages indicate concurrent deposition and subduction of fault-bounded packages (Vannucchi et al., 2008, 2012). Some outcrops display smoothly merging shear foliations at intersections of anastomosing fault strands, showing that slip was shared between them (Pasagshak, Alaska; Rodeo Cove, California). Elsewhere, we have taken the thickness of the mélange of consistent metamorphic grade as an upper limit on total fault thickness (El Cerrito Quarry, California).

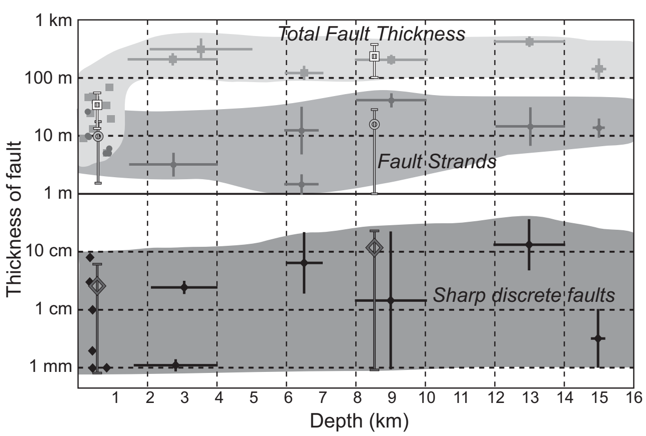

Figure 2. Thickness of total fault zone, each individual fault strand, and discrete slip surfaces plotted relative to depth of activity in kilometers (measured below seafloor for ocean drilling observations; estimated from lithostatic pressure for geologic observations). Open symbols show average and 1σ around mean for 0–1 km and 2–15 km depth populations.

The observations show two significant patterns (Fig. 2). First, there is no systematic change in the thickness of fault strands or sharp discrete faults with depth. The thickness of a single fault strand is highly variable near the trench, and the variability is consistent to 15 km. Sharp discrete faults may be underreported, as smaller features are more vulnerable to destruction or loss due to incomplete core recovery. However, the measurements made from ocean drilling in active décollements span the range of measurements from outcrop studies of ancient faults (Fig. 2), so it is likely that this variability exists from the trench to ~15 km depth.

Second, faults develop at the seafloor as a single strand and grow by developing additional separated fault strands, not through a gradual or continuous increase in thickness. This transition to a multistrand structure occurs at 1–2 km depth. We include subduction thrusts of different ages, thermal structures, convergence rates, dips, and lithologies (see the GSA Data Repository[1]). These factors influence pore pressure, deformation mechanism, and porosity response to shearing, all of which probably ultimately control strain hardening or weakening and the tendency of faults to broaden with shear. However, the remarkable consistency across ~2–15 km depth suggests that the 100–350-m-thick multistrand fault is sufficiently weak relative to the prism and the oceanic plate that gradual growth is discouraged. The mature fault zone is about an order of magnitude thicker than an individual fault strand.

CONSEQUENCES OF CONSISTENT THICKNESS WITH DEPTH

Strain localization may increase with slip rate (Chester and Chester, 1998; Ujiie and Tsutsumi, 2010), and the records of the highest strain rates (indicated by evidence of flash heating) are found on thin fault surfaces. Broadening of slipping zones may be favored in strain-hardening materials including clay-rich sediments (Faulkner et al., 2008). Thicker fault strands that contain and are cut by contemporaneous sharp discrete faults may deform at slip rates ranging from plate rate to seismic (~1 m/s), although these fast slip rates cannot be detected on thicker faults (Rowe et al., 2011). The studied faults range from ~0 to 15 km depth, at temperatures of fault activity to ~250–300 °C (see the Data Repository). At these temperatures, granular flow and/or cataclasis and solution creep are the dominant deformation mechanisms. The rate of solution creep increases with temperature, increasing in relative importance in accommodating plate motion with depth. At temperatures above ~300–350 °C, the onset of crystal plastic deformation in quartz and feldspar might change the deformation regime and the effective width of faults.

This compilation may also be compared to models for exhumation of high-pressure–low-temperature metamorphic rocks that require upward backflow of buoyant low-density sediments along the décollement (Cloos and Shreve, 1988). All of the examples include reports of fault kinematics, and they are universally consistent with seaward-vergent overthrusting. There is no evidence for upward flow of material in the fault zones, as has been suggested for Franciscan mélanges at similar pressure-temperature conditions. This does not rule out buoyant backflow at greater depths, but it does show that the necessary conditions to allow such flow are not a universal condition in the mid-seismogenic zone. We place a limit of ~100–350 m on the reasonable width that could be used to model such channel flow in the seismogenic zone (we see no thickening with depth below ~1–2 km as predicted by Cloos and Shreve, 1988, or Moore and Byrne, 1987).

SUBDUCTION THRUST FAULTS COMPARED TO CONTINENTAL FAULTS

Compilations of damage zone width in continental faults by Mitchell and Faulkner (2009) and Savage and Brodsky (2011) indicate increasing width with displacement until ~200–400 m wide at ~150 m of offset, followed by slower but continued growth. In mature faults, a zone of low seismic velocity around the fault has been correlated to the width of the active zone, and these have been estimated as ~100–400 m and 150–200 m wide (San Andreas fault; Huang and Ampuero, 2011; Yang et al., 2011). Varying definitions of fault zone and damage zone widths are used in these studies, so it is interesting to see that they report similar dimensions to the total fault width in this study (Fig. 2).

Our subduction compilation shows a stable fault width at ~1–2 km depth or ~5–12 km displacement (assuming dips of 2°–10°), which is 1–2 orders of magnitude more slip than the continental faults take to reach mature width. This slow growth may be attributable to underconsolidation, granular flow, and compaction contributing to healing deformation bands, and other particular behaviors of subducting sediments. In contrast, nonrecoverable fracturing of continental rock may more rapidly establish a permanent weak zone relative to surrounding rocks, favoring reactivation rather than expansion of the fractured zone. The threshold of ~1–2 km depth may correspond to a critical compaction at which the materials of the décollement become sufficiently stiff or impermeable to create an equivalent rheologic contrast. According to the definitions in this paper, the subduction thrust structure is more akin to the accumulated overlapping coeval strands (Childs et al., 2009; Savage and Brodsky, 2011) than to a model for damage zone growth by near-fault fracturing around a dominant slipping strand (e.g., Shipton and Cowie, 2001).

CONCLUSION

At depths <1–15 km, subduction plate boundary faults consist of one or more strands 5–35 m thick, cut by sharp discrete faults <1–20 cm wide, that accommodated highly localized slip (including, but not limited to, earthquake slip). At shallow depths there may be only one fault strand, but at depths >1–2 km, faults develop multiple strands tens of meters thick that anastomose through a zone ~100–350 m thick. The thickness of this zone does not increase down to ~15 km depth. For the purpose of dynamic and fluid flow modeling, the effective deforming width of subduction faults during slow slip or creep should be one or more strands ~5–35 m thick, bounding less deformed rock, within a total thickness of 100–350 m, and some of the interseismic permanent deformation being taken up over broader regions of wall rock.

ACKNOWLEDGMENTS

We thank John Wakabayashi for helpful conversations and permission to use his measurements of the El Cerrito Quarry fault (California). We thank Dan Faulkner, Gaku Kimura, an anonymous reviewer, and editor Bob Holdsworth for thorough and thoughtful suggestions that improved this paper. We are grateful for the assistance of the scientific and drilling staff on Drilling Vessel *Chikyu*. This work was supported by the Natural Sciences and Engineering Research Council of Canada (NSERC) Discovery Grants Program (Rowe) and the U.S. Science Support Program (Moore).

REFERENCES CITED

Bangs, N.L., Shipley, T.H., Gulick, S.P.S., Moore, G.F., Kuromoto, S., and Nakamura, Y., 2004, Evolution of the Nankai Trough décollement from the trench into the seismogenic zone: Inferences from three-dimensional seismic reflection imaging: Geology, v. 32, p. 273–276, doi:10.1130/G20211.2.

Chester, F.M., and Chester, J.S., 1998, Ultracataclasite structure and friction processes of the Punchbowl fault, San Andreas system, California: Tectonophysics, v. 295, p. 199–221, doi:10.1016/S0040-1951(98)00121-8.

Chester, F.M., Mori, J.J., Toczko, S., Eguchi, N., and the Expedition 343/343T Scientists, 2012, Japan Trench Fast Drilling Project (JFAST): Integrated Ocean Drilling Program Preliminary Report, v. 343/343T, doi:10.2204/iodp.pr.343343T.2012.

Childs, C., Manzocchi, T., Walsh, J.J., Bonson, G., Nicol, A., and Schöpfer, M.P.J., 2009, A geometric model of fault zone and fault rock thickness variations: Journal of Structural Geology, v. 31, p. 117–127, doi:10.1016/j.jsg.2008.08.009.

Cloos, M., and Shreve, R.L., 1988, Subduction-channel model of prism accretion, mélange formation, sediment subduction, and subduction erosion at convergent plate margins: 1. Background and description: Pure and Applied

[1]GSA Data Repository item 2013277, details of compiled fault measurements from Ocean Drilling Program and outcrop studies, is available online at www.geosociety.org/pubs/ft2013.htm, or on request from editing@geosociety.org or Documents Secretary, GSA, P.O. Box 9140, Boulder, CO 80301, USA.

Geophysics, v. 128, p. 455–500, doi:10.1007/BF00874548.

Cowan, D.S., 1978, Origin of blueschist-bearing chaotic rocks in the Franciscan Complex, San Simeon, California: Geological Society of America Bulletin, v. 89, p. 1415–1432, doi:10.1130/0016-7606(1978)89<1415:OOBCRI>2.0.CO;2.

Expedition 316 Scientists, 2009, Expedition 316 Site C0007, *in* Kinoshita, M., et al., eds., Proceedings of the Integrated Ocean Drilling Program, Leg 314/315/316: Washington, D.C., Integrated Ocean Drilling Program Management International, Inc., doi:10.2204/iodp.proc.314315316.135.2009.

Fagereng, Å., 2013, On stress and strain in a continuous-discontinuous shear zone undergoing simple shear and volume loss: Journal of Structural Geology, v. 50, p. 44–53, doi:10.1016/j.jsg.2012.02.016.

Faulkner, D.R., Mitchell, T.M., Rutter, E.H., and Cembrano, J., 2008, On the structure and mechanical properties of large strike-slip faults, *in* Wibberley, C.A.J., et al., eds., The internal structure of fault zones: Implications for mechanical and fluid-flow properties: Geological Society of London Special Publication 299, p. 139–150, doi:10.1144/SP299.9.

Huang, Y., and Ampuero, J.-P., 2011, Pulse-like ruptures induced by low-velocity fault zones: Journal of Geophysical Research, v. 116, B12307, doi:10.1029/2011JB008684.

Ikesawa, E., Sakaguchi, A., and Kimura, G., 2003, Pseudotachylyte from an ancient accretionary complex: Evidence for melt generation during seismic slip along a master décollement?: Geology, v. 31, p. 637–640, doi:10.1130/0091-7613(2003)031<0637:PFAAAC>2.0.CO;2.

Ikesawa, E., Kimura, G., Sato, K., Ikehara-Ohmori, K., Kitamura, Y., Yamaguchi, A., Ujiie, K., and Hashimoto, Y., 2005, Tectonic incorporation of the upper part of oceanic crust to overriding plate of a convergent margin: An example from the Cretaceous–early Tertiary Mugi Mélange, the Shimanto Belt, Japan: Tectonophysics, v. 401, p. 217–230, doi:10.1016/j.tecto.2005.01.005.

Kimura, G., Yamaguchi, A., Hojo, M., Kitamura, Y., Kameda, J., Ujiie, K., Hamada, Y., Hamahashi, M., and Hina, S., 2012, Tectonic mélange as a fault rock of subduction plate boundary: Tectonophysics, v. 568–569, p. 25–38, doi:10.1016/j.tecto.2011.08.025.

Meneghini, F., and Moore, J.C., 2007, Deformation and hydrofracture in a subduction thrust at seismogenic depths: The Rodeo Cove thrust zone, Marin Headlands, California: Geological Society of America Bulletin, v. 119, p. 174–183, doi:10.1130/B25807.1.

Mitchell, T.M., and Faulkner, D., 2009, The nature and origin of off-fault damage surrounding strike-slip fault zones with a wide range of displacements: A field study from the Atacama fault system, northern Chile: Journal of Structural Geology, v. 31, p. 802–816, doi:10.1016/j.jsg.2009.05.002.

Moore, J.C., and Byrne, T., 1987, Thickening of fault zones: A mechanism of mélange formation in accreting sediments: Geology, v. 15, p. 1040–1043, doi:10.1130/0091-7613(1987)15<1040:TOFZAM>2.0.CO;2.

Remitti, F., Vannucchi, P., and Bettelli, G., 2007, Internal structure and tectonic evolution of an underthrust tectonic mélange: The Sestola-Vidiciatico tectonic unit of the Northern Apennines, Italy: Geodinamica Acta, v. 20, p. 37–51, doi:10.3166/ga.20.37-51.

Rowe, C.D., Meneghini, F., Moore, J.C., and McKiernan, A.W., 2005, Large-scale pseudotachylytes and fluidized cataclasites from an ancient subduction thrust fault: Geology, v. 33, p. 937–940, doi:10.1130/G21856.1.

Rowe, C.D., Meneghini, F., and Moore, J.C., 2011, Textural record of the seismic cycle: Strain-rate variation in an ancient subduction thrust, *in* Fagereng, Å., et al., eds., Geology of the earthquake source: A volume in honour of Rick Sibson: Geological Society of London Special Publication 359, p. 77–95, doi:10.1144/SP359.5.

Sakaguchi, A., 2003, Tectonic setting of seismic faulting characterized by repeated pseudotachylyte formation in an ancient subduction zone, Okitsu Melange, Shimanto accretionary complex, SW Japan: Frontier Research on Earth Evolution, v. 1, p. 175–180.

Savage, H.M., and Brodsky, E.E., 2011, Collateral damage: Evolution with displacement of fracture distribution and secondary fault strands in fault damage zones: Journal of Geophysical Research, v. 116, B03405, doi:10.1029/2010JB007665.

Segall, P., and Rice, J.R., 1995, Dilatancy, compaction, and slip instability of a fluid-infiltrated fault: Journal of Geophysical Research, v. 100, p. 22,155–22,171, doi:10.1029/95JB02403.

Shipboard Scientific Party, 1988, Site 671 and Site 676, *in* Mascle, A., and Moore, J.C., et al., eds., Proceedings of the Ocean Drilling Program, Initial Reports, Leg 110, Part A: College Station, Texas, Ocean Drilling Program, p. 67–204 and p. 509–573.

Shipboard Scientific Party, 1991, Site 808, *in* Taira, A., et al., eds., Proceedings of the Ocean Drilling Program, Initial reports, Leg 131: College Station, Texas, Ocean Drilling Program, p. 71–269, doi:10.2973/odp.proc.ir.131.106.1991.

Shipboard Scientific Party, 1997, Site 1043, *in* Kimura, G., et al., eds., Proceedings of the Ocean Drilling Program, Initial reports, Leg 170: College Station, Texas, Ocean Drilling Program, p. 215–247, doi:10.2973/odp.proc.ir.170.107.1997.

Shipboard Scientific Party, 1998, Site 1044, Site 1045, Site 1046, and Site 1047, *in* Moore, J.C., Klaus, A., et al., eds., Proceedings of the Ocean Drilling Program, Initial Reports, Leg 171A: College Station, Texas, Ocean Drilling Program, p. 19–91.

Shipboard Scientific Party, 2002, Leg 196 summary: Deformation and fluid flow processes in the Nankai Trough accretionary prism: Logging while drilling and Advanced CORKs, *in* Mikada, H., et al., eds., Proceedings of the Ocean Drilling Program, Initial reports, Leg 196: College Station, Texas, Ocean Drilling Program, p. 1–29, doi:10.2973/odp.proc.ir.196.101.2002.

Shipboard Scientific Party, 2003, Site 1254, *in* Morris, J.D., et al., eds., Proceedings of the Ocean Drilling Program, Initial reports, Leg 205: College Station, Texas, Ocean Drilling Program, p. 1–113, doi:10.2973/odp.proc.ir.205.105.2003.

Shipboard Scientific Party, 2009, Expedition 316 Site C0007, *in* Kinoshita, M., et al., eds., Proceedings of the Ocean Drilling Program, Initial reports, Leg 314/315/316: College Station, Texas, Ocean Drilling Program, p. 1–110.

Shipley, T.H., Moore, G.F., Bangs, N.L., Moore, J.C., and Stoffa, P.L., 1994, Seismically inferred dilatancy distribution, northern Barbados Ridge décollement: Implications for fluid migration and fault strength: Geology, v. 22, p. 411–414, doi:10.1130/0091-7613(1994)022<0411:SIDDNB>2.3.CO;2.

Shipton, Z.K., and Cowie, P.A., 2001, Damage zone and slip-surface evolution over μm to km scales in high-porosity Navajo sandstone, Utah: Journal of Structural Geology, v. 23, p. 1825–1844, doi:10.1016/S0191-8141(01)00035-9.

Sibson, R.H., 2003, Thickness of the seismic slip zone: Seismological Society of America Bulletin, v. 93, p. 1169–1178, doi:10.1785/0120020061.

Sleep, N.H., and Blanpied, M.L., 1992, Creep, compaction and the weak rheology of major faults: Nature, v. 359, p. 687–692, doi:10.1038/359687a0.

Ujiie, K., and Tsutsumi, A., 2010, High-velocity frictional properties of clay-rich fault gouge in a megasplay fault zone, Nankai subduction zone: Geophysical Research Letters, v. 37, L24310, doi:10.1029/2010GL046002.

Ujiie, K., Yamaguchi, A., Kimura, G., and Toh, S., 2007a, Fluidization of granular material in a subduction thrust at seismogenic depths: Earth and Planetary Science Letters, v. 259, p. 307–318, doi:10.1016/j.epsl.2007.04.049.

Ujiie, K., Yamaguchi, H., Sakaguchi, A., and Toh, S., 2007b, Pseudotachylytes in an ancient accretionary complex and implications for melt lubrication during subduction zone earthquakes: Journal of Structural Geology, v. 29, p. 599–613, doi:10.1016/j.jsg.2006.10.012.

Vannucchi, P., Remitti, F., and Bettelli, G., 2008, Geological record of fluid flow and seismogenesis along an erosive subducting plate boundary: Nature, v. 451, p. 699–703, doi:10.1038/nature06486.

Vannucchi, P., Sage, F., Phipps Morgan, J., Remitti, F., and Collot, J.-Y., 2012, Toward a dynamic concept of the subduction channel at erosive convergent margins with implications for interplate material transfer: Geochemistry Geophysics Geosystems, v. 13, Q02003, doi:10.1029/2011GC003846.

Wakabayashi, J., 2011, Mélanges of the Franciscan Complex, California: Diverse structural settings, evidence for sedimentary mixing, and their connection to subduction processes, *in* Wakabayashi, J., and Dilek, Y., eds., Mélanges: Processes of formation and societal significance: Geological Society of America Special Paper 480, p. 117–141, doi:10.1130/2011.2480(05).

Wakabayashi, J., 2013, Subduction initiation, accretion and nonaccretion, large-scale material movement, and localization of subduction megaslip recorded in Franciscan Complex and related rocks, California, *in* Putirka, K., ed., Geologic excursions from Fresno, California, and the Central Valley: A tour of California's iconic geology: Geological Society of America Field Guide 32, p. 129–162, doi:10.1130/2013.0032(07).

Yang, H., Zhu, L., and Cochran, E.S., 2011, Seismic structures of the Calico fault zone inferred from local earthquake travel time modeling: Geophysical Journal International, v. 186, p. 760–770, doi:10.1111/j.1365-246X.2011.05055.x.

Manuscript received 10 March 2013
Revised manuscript received 1 May 2013
Manuscript accepted 2 May 2013

Printed in USA